

Spatio-temporal variability of zooplankton standing stock in  
eastern Arabian Sea inferred from ADCP backscatter  
measurements

Ranjan Kumar Sahu, P. Amol, D.V. Desai, S.G. Aparna, D. Shankar

July 4, 2024

**Abstract**

We use acoustic Doppler current profiler (ADCP) backscatter measurements to map the spatio-temporal variation of zooplankton standing stock in the eastern Arabian Sea (EAS). The ADCP moorings were deployed at seven locations on the continental slope off the west coast of India; we use data from October 2017 to December 2023. The 153.3 kHz ADCP uses backscatter from sediments or organisms such as copepods, ctenophores, salps and amphipods greater than 1 cm to calculate current profile. The backscatter is obtained from echo intensity using RSSI conversion factor after doing necessary calibrations. The conversion from backscatter to biomass is based on volumetric zooplankton sampling at the respective locations. Analysis of the data over 24 – 120 m shows that the backscatter and zooplankton biomass decrease from the upper ocean ( $215 \text{ m g}^{-3}$  biomass contour) to the lower depths. Changes are observed in the seasonal variation of the monthly

<sup>12</sup> climatology of zooplankton standing stock (integral of the biomass over 24 – 120 m water column)  
<sup>13</sup> as we move to poleward along the slope in EAS. The range of variation of standing stock is lowest  
<sup>14</sup> at Kanyakumari, followed by Okha, which lie at the southern and northern boundary of the EAS,  
<sup>15</sup> respectively. Complementary variables are used to explain the processes leading to growth or decay  
<sup>16</sup> of zooplankton biomass.

<sub>17</sub> **1 Introduction**

<sub>18</sub> **1.1 Background**

<sub>19</sub> Zooplankton plays a vital role in food web of pelagic ecosystem by enabling the hierarchical trans-  
<sub>20</sub> port of organic matter from primary producers to higher trophic levels impacting the fish population  
<sub>21</sub> and the carbon pump of the deep ocean [Ohman and Hirche, 2001, Le Qu et al., 2016]. They are  
<sub>22</sub> presumably the largest migrating organisms in terms of biomass [Hays, 2003] which occurs in diel  
<sub>23</sub> vertical migration (DVM). Zooplanktons depend not only on phytoplankton but other environ-  
<sub>24</sub> mental parameters (e.g. Mixed layer depth, insolation, Oxygen, thermocline, nutrient availability,  
<sub>25</sub> chlorophyll concentration and daily primary production). The biological productivity of the ocean  
<sub>26</sub> is essentially connected with physics and chemistry [Subrahmanyam, 1959, Ryther et al., 1966,  
<sub>27</sub> Qasim, 1977, Nair, 1970, Banse, 1995, McCreary et al., 2009, Vijith et al., 2016, Amol et al., 2020].  
<sub>28</sub> The dynamic ocean results in varying physico-chemical properties, leading to bloom and growth of  
<sub>29</sub> planktons in favourable conditions. The changes are strongly influenced by the seasonal cycle in  
<sub>30</sub> the North Indian Ocean (NIO; north of 5 °N of Indian Ocean). The eastern boundary of Arabian  
<sub>31</sub> Sea contains the West India Coastal Current (WICC; [Patil et al., 1964, Ramamirtham and Murty,  
<sub>32</sub> 1965, Banse, 1968, Shetye et al., 1991, McCreary Jr et al., 1993, Shankar and Shetye, 1997, Shetye  
<sub>33</sub> and Gouveia, 1998, Maheswaran et al., 2000, Amol et al., 2014, Chaudhuri et al., 2020, 2021])  
<sub>34</sub> which reverses seasonally, flowing poleward (equatorward) during November to February (June to  
<sub>35</sub> September).  
<sub>36</sub> The direct consequence of this reversal is the seasonal cycle of thermocline, oxycline and thick-  
<sub>37</sub> ness of mixed Layer Depth (MLD) induced by upwelling favourable conditions in summer and down-  
<sub>38</sub> welling favourable conditions in winter in eastern Arabian Sea (EAS). Further, the phytoplankton

39 biomass and chlorophyll concentration changes with the season [Subrahmanyam and Sarma, 1960,  
40 Banse, 1968, Lévy et al., 2007, Vijith et al., 2016]. Upwelling in summer monsoon leads to maxi-  
41 mum chlorophyll growth in the entire EAS [Banse, 1968, Banse and English, 2000, McCreary et al.,  
42 2009, Hood et al., 2017]. During winter monsoon, the convective mixing induced winter mixed layer  
43 [Shetye et al., 1992, Madhupratap et al., 1996b, Lévy et al., 2007, Vijith et al., 2016, Shankar et al.,  
44 2016, Keerthi et al., 2017] results in winter chlorophyll peak in northern EAS (NEAS) while the  
45 downwelling Rossby waves modulate chlorophyll along the southern EAS (SEAS) albeit limited to  
46 coast and islands [Amol et al., 2020]. (For a detailed description on EAS division, please refer figure  
47 1 of [Shankar et al., 2019].

48 The zooplankton grazing peak is instantaneous with no time delay from peak phytoplankton  
49 production [Li et al., 2000], but its population growth lags [Rehim and Imran, 2012, Almén and  
50 Tamelander, 2020] depending on its gestation period and other limiting aspects. While some studies  
51 suggest that the peak timing of zooplankton may not change in parallel with phytoplankton blooms  
52 [Winder and Schindler, 2004], others indicate that lag exists between primary production and the  
53 transfer of energy to higher trophic levels [Brock and McClain, 1992, Brock et al., 1991]. A recent  
54 work [Aparna et al., 2022] had shown that peak zooplankton population may never occur even  
55 with a bloom in phytoplankton such as in SEAS, leading to the collapse of ecological models and  
56 succeeding food webs of higher trophic levels.

57 The conventional zooplankton measurements, where only few snapshot/s of the event is cap-  
58 tured gives an incoherent or incomplete understanding in terms of spatio-temporal variation of  
59 zooplankton [Ramamurthy, 1965, Piontkovski et al., 1995, Madhupratap et al., 1992, 1996a, Wish-  
60 ner et al., 1998] as much information is revealed by later studies [Jyothibabu et al., 2010, Vijith  
61 et al., 2016, Shankar et al., 2019, Aparna et al., 2022] using high resolution data. Calibrated acous-

tic instruments such as Acoustic Doppler Current Profiler (ADCP) along with relevant data can be utilised to understand small scale variability [Nair et al., 1999, Edvardsen et al., 2003, Smith and Madhupratap, 2005, Smeti et al., 2015, Kang et al., 2024], the complex interplay between the physico-chemical parameters and ecosystem [Jiang et al., 2007, Potiris et al., 2018, Shankar et al., 2019, Aparna et al., 2022, Nie et al., 2023], the zooplankton migration [Inoue et al., 2016, Ursella et al., 2018, 2021] and their seasonal to annual variation [Jiang et al., 2007, Hobbs et al., 2021, Liu et al., 2022, Aparna et al., 2022].

## 69    1.2 ADCP backscatter and zooplankton biomass

70    At present, there are two types of acoustic samplers: non-calibrated single frequency acoustic profiler such as ADCP or calibrated multi and mono frequency acoustic profilers such as zooplankton acoustic profiler (ZAP) and Tracor acoustic profiling system(TAPS). The use of acoustics as a proxy for zooplankton biomass estimation can be traced to [Pieper, 1971, Sameoto and Paulowich, 1977] and earlier studies which used echograms to approximate the large-scale horizontal extents [Barraclough et al., 1969], and small scale vertical extent [McNaught, 1968]. The relationship between backscatter and the abundance and size of zooplankton was described by [Greenlaw, 1979] wherein it was pointed out that single frequency backscatter can be used to estimate abundance if mean zooplankton size is known. This paved the way for use of single frequency acoustic profiler. A drastic increase in study temporal and spatial variation of zooplankton biomass using backscatter-proxy came in 1990s by introduction of high frequency echo sounders, with studies [Flagg and Smith, 1989, Wiebe et al., 1990, Batchelder et al., 1995, Greene et al., 1998, Rippeth and Simpson, 1998] methodically showing acoustic backscatter estimated zooplankton biomass in various shelf and slope locations around North Atlantic, North pacific location. The foundation for further research that

84 investigated the potential of acoustic backscatter from ADCPs and multi frequency echo sounders  
85 in assessing zooplankton biomass and comprehending zooplankton dynamics in diverse maritime  
86 habitats was established by these initial explorative experiments.

87 Acoustic backscatter and zooplankton biomass have been better understood as a result of tech-  
88 nological and methodological developments over time. Net sampling augmented ADCP backscatter  
89 have been used to study DVM and the spatial and temporal variability of zooplankton biomass by  
90 [Cisewski et al., 2010, Smeti et al., 2015, Guerra et al., 2019] in different marine regions, such as the  
91 Southwestern Pacific, the Lazarev Sea in Antarctica and the Corsica Channel in the north-western  
92 Mediterranean Sea. The zooplankton biomass variation in the Arabian sea has been studied during  
93 JGOFS programme in 1990s [Herring et al., 1998, Nair et al., 1999, Fielding et al., 2004, Smith and  
94 Madhupratap, 2005]. However, their studies were limited to the cruise duration as vessel mounted  
95 ADCPs were predominantly used; hence long-term data was sparsely produced. The first such  
96 study to fully exploit the immense potential of ADCPs in EAS was carried out by [Aparna et al.,  
97 2022] using ADCP moorings deployed on continental slopes off the Indian west coasts [Amol et al.,  
98 2014, Chaudhuri et al., 2020].

### 99 1.3 Objective and scope of the manuscript

100 A network of ADCPs has been installed off the continental slope and shelf on the west coast of  
101 India. This ADCPs have enabled a rigorous view of intraseasonal to seasonal scale variability [Amol  
102 et al., 2014, Chaudhuri et al., 2020]. Initially a network of 4 ADCPs (off Mumbai, Goa, Kollam and  
103 Kanyakumari) on continental slope, it has been extended to include 3 more moorings (off Okha from  
104 2018, Jaigarh and Udupi from 2017). In the recent study [Aparna et al., 2022] have used ADCP  
105 moorings off Mumbai, Goa and Kollam to explain the temporal variability of zooplankton biomass.

106 The study showed that the zooplankton peaks (and troughs) is not only non-uniform in latitude but  
107 also heavily influenced by the oxygen minimum zone, MLD and the seasonal upwelling/downwelling  
108 conditions. Stark contrast in the phytoplankton bloom and subsequence growth of zooplankton or  
109 the lack thereof was observed in the EAS regimes.

110 We build upon the existing work by extending to include the newly incorporated ADCPs so as to  
111 have a better understanding in the latitudinal variation of zooplankton biomass in EAS. The paper  
112 is organized as follows; datasets and methods employed are described in detail in Section 2. Section  
113 3 describes the observed climatology of zooplankton biomass and standing stock. A comparison is  
114 drawn to the results of previous studies at the overlapping mooring sites. Further, the seasonal cycle  
115 of zooplankton biomass and standing stock is discussed. The role of mixed layer depth, net primary  
116 production, sea surface temperature, wind forcing and circulation in determining the biomass is  
117 discussed in results section 4, with conclusion in section 5.

## 118 2 Data and methods

119 The backscatter data from ADCP and the zooplankton samples collected from the periphery of  
120 mooring is described in this section. The methodology followed in processing ADCP data and  
121 estimation of backscatter and subsequently the zooplankton biomass is discussed. The backscatter  
122 derived from the echo intensity of the seven ADCP mooring deployed on the continental slope off  
123 the Indian west coast is the primary data we have use in this manuscript. The moorings details are  
124 summarised in [Table 1](#). In situ biomass data from volumetric zooplankton samples are used to val-  
125 idate and correlate with backscatter. The chlorophyll data is obtained from [marine.copernicus.eu](http://marine.copernicus.eu).  
126 In addition, we have used the monthly climatology of temperature and salinity [[Chatterjee et al.,](#)  
127 [2012](#)] and the net primary productivity from MODIS (Moderate Resolution Imaging Spectrora-

128 diometer) and VIIRS (Visible Infrared Imaging Radiometer Suite) from global NPP estimates  
129 (<http://sites.science.oregonstate.edu/ocean.productivity>).

## 130 2.1 ADCP data and Backscatter estimation

131 The ADCPs were deployed on the continental slope off the Indian west coast ([Fig. 1](#)). Initially a  
132 set of three ADCPs, it was gradually extended to four more sites to cover the entire EAS basin  
133 from Okha ( $22.26^{\circ}\text{N}$ ) in north to Kanyakumari ( $6.96^{\circ}\text{N}$ ) in south. The other two ADCPs are  
134 Jaigarh at central EAS (CEAS) and Udupi in the transition zone between CEAS & SEAS. The  
135 extended moorings were deployed in October 2017, except for Kanyakumari which was deployed  
136 earlier as well but it wasn't included in earlier backscatter study. The moorings are serviced on  
137 yearly basis usually during October-November or in winter monsoon months. The ADCPs are of  
138 RD Instruments make, upward-looking and operate at 153.3 kHz. While utmost care is taken to  
139 position the instrument at  $\sim 200$  m depth, yet for some deployments it's shallow or deeper owing  
140 to drift caused by floater buoyancy - anchor weight balance. Data was collected at hourly interval  
141 and the bin size was set to 4 m. The echoes at surface to 10 % range ( 20 m) means the data at  
142 these is rendered useless and is discarded from further use.

143 The procedure followed in processing of the ADCP data are described in [[Amol et al., 2014](#)]  
144 and [[Mukherjee et al., 2014](#)]. An addition to their methodology was to do depth correction to ac-  
145 commodate the vertical movement of ADCP buoys [[Chaudhuri et al., 2020](#), [Mukhopadhyay et al.,](#)  
146 [2020](#)] using data from pressure sensor mounted on the instrument. We have followed the method-  
147 ology laid down in [[Aparna et al., 2022](#)] to derive the backscatter time series from ADCP echo  
148 intensity data which is discussed later paragraph. The gaps are filled using the grafting method of  
149 [[Mukhopadhyay et al., 2020](#)] once the zooplankton biomass time series is constructed.

150        The primary objective of ADCP usage is to obtain vertical current profile at a point location. It  
151        is achieved by using the echo intensity received at the ADCP transducer. The instrument sensors  
152        doesn't directly give backscatter, as echo intensity is range independent. Range correction has to  
153        be performed before echo intensity (E) is converted to Backscatter (B). Received signal strength  
154        indicator (RSSI), also called the conversion factor (Kc) which is specific to a sensor is used along with  
155        the corresponding reference echo intensity (Er). It's important to state that for the same device Kc  
156        remains unchanged while Er varies over each subsequent deployment. The backscattering strength  
157        (in dB) is given by [Mullison, 2017]:

$$158 \quad B = [C - L_{DBM} - P_{DBW}] + 2\alpha R + 10\log_{10}[(T_{TD} + 273.16)R^2] + 10\log_{10}[10^{K_c(E-E_r)/10} - 1]$$

159        where  $C$  is an empirical constant,  $L_{DBM}$  is  $10\log_{10}L$  where  $L$  is the transmit pulse length in  
160        meters,  $P_{DBW}$  is  $10\log_{10}P$  ( $P$  is transmitted power in watts),  $\alpha$  is the sound absorption coefficient  
161        of water (in  $dB m^{-1}$ ),  $T_{TD}$  is the temperature (in  ${}^\circ C$ ) at the depth of positioned instrument,  $R$   
162        is the slant range (in meters) from transducer to the scatterers and  $E_r$  is the reference level of  $E$   
163        taken in real-time (unit counts).  $E_r$  in our case is taken from first (last) measured profile when the  
164        instrument is in air before (after) deployment (retrieval). The backscattering strength is referenced  
165        to  $(4\pi m^{-1})$  [Deines, 1999, Mullison, 2017]. Aparna et al. [2022] has discussed the relevance of each  
166        of the term to the total backscattering strength. Our analysis also suggests that the  $\alpha$  does not  
167        affect the final results.

## 168        2.2 Zooplankton data and estimation of biomass

169        The zooplankton samples were collected in the vicinity ( $\sim 10$  km) of ADCP mooring site twice; once  
170        prior retrieval and again post deployment of moorings so that there is overlap in the ADCP time  
171        instance and in situ zooplankton samples. The sampling is done at the mooring location during

<sup>172</sup> servicing cruises on board RV Sindhu Sankalp and RV Sindhu Sadhana (Table 2). Multi-plankton  
<sup>173</sup> net (MPN) (100  $\mu\text{m}$  mesh size, 0.5  $\text{m}^2$  mouth area) was used to get samples in the pre-determined  
<sup>174</sup> depth ranges; water volume filtered was calculated by the product of sampling depth range and the  
<sup>175</sup> mouth area of net. The depth range and timing of sample collection was different throughout the  
<sup>176</sup> MPN hauls (refer [Table 2](#)). From 2020 onward, the depth-range was standardized to the bins of 0  
<sup>177</sup> - 25, 25 - 50, 50 - 75, 75 - 100, 100 - 150 (units are in meters). The collected zooplankton samples  
<sup>178</sup> were then preserved in 5 % formaldehyde solution until it's transferred to laboratory. To measure  
<sup>179</sup> zooplankton wet weight accurately, the gelatinous forms/salps were separated. [[Aparna et al.,](#)  
<sup>180</sup> [2022](#)] had reported the calanoid copepods, cyclopoid copepods, Poecilostomatoida, Harpacticoida,  
<sup>181</sup> appendicularians, euphausids, ostracods, and chaetognaths as the major groups of zooplanktons  
<sup>182</sup> contributing to the biomass of net samples from the mooring sites. The backscatter obtained earlier  
<sup>183</sup> is averaged in vertical corresponding to the specific MPN hauls for each site. The backscatter is  
<sup>184</sup> linear regressed with respective biomass to establish their relationship, which has been demonstrated  
<sup>185</sup> in numerous previous studies [[Flagg and Smith, 1989](#), [Heywood et al., 1991](#), [Jiang et al., 2007](#),  
<sup>186</sup> [Aparna et al., 2022](#)].

<sup>187</sup> We calculated the regression equation to be  $y = 0.0203 x + 4.01$  and, which is well within the  
<sup>188</sup> error range of the regression equation of [[Aparna et al., 2022](#)],  $y = (0.02 \pm 0.004) x + (4.14 \pm 0.36)$   
<sup>189</sup> with a correlation of 0.53 ([Fig. 2](#)). The correlation value in our case is 0.54; the minor difference is  
<sup>190</sup> due to higher number of data points (159) in the present study.

### <sup>191</sup> **2.3 Biomass time series and estimation of standing stock**

<sup>192</sup> The zooplankton biomass time series ([Fig. 3](#)) is created from the above derived linear relationship:  
<sup>193</sup>  $\log_{10}(\text{biomass}) = m * \text{Backscatter} + k$ , where  $m$  is slope and  $k$  is intercept. The time series shows

194 the pattern of diel vertical migration (DVM) at all the mooring sites during dawn ( $\sim$ 0600-0700  
195 hours) and dusk ( $\sim$ 1800-1900 hours). It is evident in earlier studies using backscatter [Ashjian  
196 et al., 2002, Smith and Madhupratap, 2005, Inoue et al., 2016, Ursella et al., 2018] and in situ  
197 zooplankton data [Padmavati et al., 1998]. The implication of DVM is a higher biomass at surface  
198 during the night as zooplankton feeds and a lower biomass at daytime as they descend to subsurface  
199 depths. The overall biomass over the time period of a day may vary but the DVM doesn't affect  
200 the seasonal variation as shown by ([Jiang et al., 2007, Aparna et al., 2022]). Since our goal is to  
201 study the seasonal variation, delineating the daily biomass is sufficient. The biomass time series  
202 and seasonal cycle is discussed in ??.

203 The standing stock is determined by taking the depth integral of biomass over the water column.  
204 To maintain the consistency of standing stock estimation, only those deployments that doesn't lack  
205 data at any depth in the entire range of 24 - 120 m are considered for analysis. The lack of data in  
206 the above mentioned depth range is due to deviation in positioning of ADCP sensor in the water  
207 column. A swift alteration in bathymetry along the continental slope implies that the mooring  
208 might anchor at a different depth than planned, hence a change in the predicted position of ADCP.  
209 This leads to gap in data at few mooring sites for some year. For example, for the northern-most  
210 mooring at Okha, data is not available for the entire upper 120 m depth for the second deployment.  
211 Also at Jaigarh, where the surface to  $\sim$ 60m data (in 3rd deployment) and Kollam, where 80 m  
212 and below (in 4th deployment) is unavailable and hence discarded from standing stock estimation.  
213 There are few deployments where no data or bad data was recorded e.g, at Udupi (4th deployment)  
214 and Kanyakumari (6th deployment). The seasonal cycle of standing stock for 24 - 120 m available  
215 data is explored in subsection 4.1.

216 **2.4 Mixed-layer depth, temperature and oxygen**

217 As we are using a 153.3 kHz ADCP moored at  $\sim$  150 m, the top  $\sim$  10% of data is unusable  
218 because of surface echoes. MLD in EAS is of the order  $\sim$  20 to 40 m during summer monsoon  
219 [Shetye et al., 1990, Sreenivas et al., 2008] especially in the SEAS. Although it is possible to use  
220 the near surface ADCP data after due noise correction; it is beyond the scope of present study.  
221 The temperature data is used from [Chatterjee et al., 2012] which is a monthly climatology having  
222  $1^{\circ}$  spatial resolution. Monthly climatology of oxygen data is obtained from World Ocean Atlas  
223 2013 [García et al., 2014] which contains objectively analyzed  $1^{\circ}$  climatological fields of in situ  
224 measurements.

225 **2.5 Chlorophyll and net primary productivity data**

226 Previous study based on ADCP data of EAS [Aparna et al., 2022] have used SeaWiFS based chloro-  
227 phyll data for comparison with climatology of zooplankton standing stock (ZSS). The SeaWiFS was  
228 at its end of service in 2010, hence we use new chlorophyll product. The present study has been  
229 conducted using Global Ocean Colour, biogeochemical, L3 data obtained from the [E.U. Copernicus](#)  
230 [Marine Service Information](#). The daily data is available at a spatial resolution of 4 km.

231 While chlorophyll is used to compare with the variation in climatology of zooplankton standing;  
232 the growth efficiencies of zooplankton are directly linked to primary production levels, emphasizing  
233 the interconnectedness between primary producers and consumers in marine food webs [?]. In  
234 their study, [Aparna et al., 2022] has emphasized on the collapse of the predator-prey relationship  
235 between zooplankton-phytoplankton using climatological data. We showcase their interdependency  
236 or the lack thereof using net primary productivity models. Moderate Resolution Imaging Spectro-  
237 radiometer (MODIS) based net primary productivity (NPP) data at a resolution of  $0.16^{\circ} \times 0.16^{\circ}$

238 was obtained from Oregon State University. They have employed three different schemes to obtain  
239 NPP from Chlorophyll concentration. Those are discussed below in brief. The first is Vertically  
240 Generalized Production Model (VGPM). The NPP (a rate term) is to be derived from chlorophyll  
241 (a standing stock) using chlorophyll-specific assimilation efficiency for carbon fixation. The single  
242 biggest unknown in all models based on chlorophyll is how this rate term is described. VGPM  
243 considers the primary productivity to be dependent on day length and maximum daily NPP within  
244 a water column. The second is Carbon-based Productivity Model (CbPM) which NPP to phy-  
245toplankton carbon biomass and growth rate. The third is Carbon, Absorption, and Fluorescence  
246 Euphotic-resolving (CAFE) mode; first described by [Silsbe et al., 2016] takes various other factors  
247 into NPP calculations. We explore these NPP models and try to explain the variation in ZSS.

### 248 3 Climatology of zooplankton biomass and standing stock

249 The previous study of zooplankton in EAS based on ADCP backscatter was consisting of three  
250 sites: Mumbai in NEAS, Goa in CEAS and Kollam in SEAS. The extended mooring sites are at  
251 Okha at NEAS, Jaigarh at CEAS, Udupi in the transition zone of CEAS & SEAS and Kanyakumari  
252 at SEAS is the southern most location in our study area.

253 ADCP data from three mooring sites were analysed from 2012 to 2020 in [Aparna et al., 2022].  
254 They have fine-tuned the methodology to obtain backscatter and estimated zooplankton biomass  
255 from it using in situ volumetric zooplankton biomass data. A comparison is made in later para-  
256 graphs, since the methodology remains same in the current study and new time series data is  
257 available. The monthly climatology of biomass and ZSS is computed for all locations having valid  
258 data in 24 - 120 m depth range ([Fig. 4](#)).

259 The high biomass regime in the upper ocean and low biomass regime in deeper depths is dif-

260 ferentiated using a biomass contour:  $215 \text{ mg m}^{-3}$  off Mumbai, Goa and Kollam;  $200 \text{ mg m}^{-3}$  off  
261 Jaigarh and Udupi;  $175 \text{ mg m}^{-3}$  off Okha and Kanyakumari. For simplicity, this biomass contour  
262 is abbreviated to be z215, z200 & z175 and its depth is denoted as D215, D200 & D175, respec-  
263 tively. The choice of biomass contour isn't abrupt; firstly, it is carefully chosen to accommodate the  
264 seasonal variation, as a shift to biomass contour lower than the z215 would be unviable as our data  
265 is only till 140 m depth as in the case of Kollam. A higher biomass contour would lead to inferior  
266 view of the seasonal cycle such as in the case of Kanyakumari and Okha where  $215 \text{ mg m}^{-3}$  biomass  
267 contour is often low enough to reach  $\sim 20 - 30$  m depths, hence z175 is chosen here. Secondly, it  
268 allows us to link the seasonal variation of biomass to the physico-chemical properties.

269 The climatology of zooplankton biomass ([Fig. 4](#)) is discussed at locations northward starting  
270 from southernmost mooring site off Kanyakumari.

### 271 **3.1 Southern EAS**

272 At Kanyakumari, with the advent of summer monsoon, the depth of  $23^{\circ}\text{C}$  isotherm (henceforth  
273 D23) shallows along-with oxycline (marked by  $2.1 \text{ ml L}^{-1}$ ) and a rise in biomass is observed ([Fig. 4](#)  
274 g1). The z175 is shallower during June to September and the zooplankton biomass is comparatively  
275 higher than rest of the year. The D175 deepens starting from October and the relatively high  
276 biomass in water column is maintained till late December. However, this increase in D175 isn't  
277 reflected as an increase in ZSS because of low biomass in the entire water column. A gradual  
278 increase is seen in the chlorophyll biomass starting from April and the peak is attained in June  
279 ([Fig. 4 g2](#)). The ZSS is increased in June, however the growth is minimal. There is almost no  
280 seasonal variation in ZSS off Kanyakumari (seasonal ZSS range,  $2.67 \text{ gm m}^{-2}$ ) as compared to the  
281 ZSS variation at the nearest northern mooring site off Kollam (seasonal ZSS range,  $4.86 \text{ gm m}^{-2}$ ),

<sup>282</sup> where a strong seasonal cycle is observed and the D215 is deeper for any given month.

<sup>283</sup> Off Kollam, a higher biomass is present in the larger portion of water column and the D215 is  
<sup>284</sup> at  $\sim 110$  m during Mar-May ([Fig. 4 f1](#)). Similar to z175 off Kanyakumari, the decrease in biomass  
<sup>285</sup> with depth is subtle below z215. The D215 begins to shallow with progressing summer monsoon.  
<sup>286</sup> During this period, a sharp decrease is seen in the D23 ( $\sim 60$  m in June to September) while  
<sup>287</sup> the oxycline ( $1.7 \text{ ml L}^{-1}$ ) overshoots the thermocline ([Fig. 4. f1](#)). A steep rise in chlorophyll  
<sup>288</sup> biomass is seen off Kollam and its peak is attained in August ([Fig. 4 f2](#)). The ZSS declines in the  
<sup>289</sup> same period and reaches a minimum when the chlorophyll biomass is at its peak. The chlorophyll  
<sup>290</sup> biomass decreases rapidly in the following months, while the ZSS increases and a maximum is seen  
<sup>291</sup> during October. This feature was earlier reported by [[Aparna et al., 2022](#)] showing disproportionate  
<sup>292</sup> interaction between zooplankton and phytoplankton. It begs the question of existing understanding  
<sup>293</sup> of predator - prey relationship in a local-scale ecological system. A similar feature is seen further  
<sup>294</sup> north, off Udupi which sits at the transition zone of SEAS & CEAS, albeit with a relatively weaker  
<sup>295</sup> zooplankton biomass. The peak of chlorophyll and minimum of ZSS occurs in September ([Fig. 4 e2](#))  
<sup>296</sup> which is one month later than off Kollam. The  $2.1 \text{ ml L}^{-1}$  oxygen contour overshoots thermocline,  
<sup>297</sup> however it reaches to a much shallow depth of  $\sim 20$  m during July to October. The D200 closely  
<sup>298</sup> follows D23; with the gradual shallowing from March onward reaching  $\sim 60$  m in September and a  
<sup>299</sup> steep decline afterwards till November ([Fig. 4 e1](#)). Decrease in biomass with depth is moderate in  
<sup>300</sup> comparison to Kollam.

### <sup>301</sup> 3.2 Central EAS

<sup>302</sup> Off Goa, the D215 seasonal trend is similar to Udupi and is entirely restricted by D23 & oxycline  
<sup>303</sup> that closely follows it. During March-May, the D215 is at  $\sim 100$  m which shallows with onset of

<sup>304</sup> summer monsoon ([Fig. 4 d1](#)); the chlorophyll biomass increases during this period and the maximum  
<sup>305</sup> occurs in August after which the chlorophyll biomass and ZSS ([Fig. 5](#)) both decrease in September.  
<sup>306</sup> Although we witness an increase in chlorophyll biomass in October, the D215 is restricted to the  
<sup>307</sup> ~ 50 m in this period and the ZSS is at its minimum similar to what is observed off Udupi and  
<sup>308</sup> Kollam. The ZSS rapidly increases and reaches its maximum in January, sustained till March and  
<sup>309</sup> then gradually declines. Unlike the previous locations, the biomass off Goa decreases rapidly below  
<sup>310</sup> the z215 as reported earlier [[Aparna et al., 2022](#)], reaching as low as  $60 \text{ mg m}^{-3}$  during June to  
<sup>311</sup> September at 130 m ([Fig. 4 d1](#)).

<sup>312</sup> The ZSS off Jaigarh is identical but stronger to that off Goa, owing to an higher biomass above  
<sup>313</sup> z200 and the comparatively deeper D200 ([Fig. 4 c1](#)). The D200 follows D23 & oxycline for most  
<sup>314</sup> of the year and it only exceeds during October-December. From the ZSS maximum in February  
<sup>315</sup> ([Fig. 4 c2](#)), it steadily decreases and attains a minimum in September (coincides with lower D200),  
<sup>316</sup> a rapid rise is seen in the following months. What's intriguing is a presence of strong seasonal cycle  
<sup>317</sup> in ZSS off Jaigarh ( $10.38 \text{ gm m}^{-2}$ , highest among all locations) although the seasonal variation in  
<sup>318</sup> chlorophyll biomass ([Fig. 4 c2](#)) is visibly non-existent ( $0.15 \text{ mg m}^{-3}$ , lowest among all locations).  
<sup>319</sup> This is an exact opposite scenario of Kanyakumari site, where an insignificant seasonal variation in  
<sup>320</sup> ZSS ( $2.67 \text{ gm m}^{-2}$ ) is seen even though the chlorophyll biomass varies strongly ( $1.62 \text{ mg m}^{-3}$ ).

<sup>321</sup> Starting from Kollam ([Fig. 4 f1](#)) and moving northward to Jaigarh ([Fig. 4 c1](#)), we see that the  
<sup>322</sup> core of high zooplankton biomass gradually shifts from summer monsoon (off Kollam) to winter  
<sup>323</sup> monsoon (off Jaigarh), with the transition of upper ocean zooplankton biomass happening along  
<sup>324</sup> Udupi and Goa.

325 **3.3 Northern EAS**

326 Further north of Jaigarh, off Mumbai the D215 follows a similar pattern i.e, a deeper D215 in  
327 December to early April, resulting in a higher ZSS in the same period ([Fig. 4 b2](#)). The D23 off  
328 Mumbai follows D215 and the oxycline follows an erratic pattern, reaching depths > 140 during  
329 January to March ([Fig. 4 b1](#)); when a higher biomass is observed above z215. The chlorophyll  
330 biomass shows seasonal variation albeit lower than the SEAS counterpart. Its peak occurs in  
331 August, then decreases rapidly and increases from October onward maintaining the biomass at 0.5  
332  $mg\ m^{-3}$  till March. In zooplankton biomass climatology, during September-October a thin layer  
333 of low biomass regime is seen at depths ~30 - 40 m, combined with shallow D215 resulting in a  
334 ZSS minimum. The ZSS increases rapidly from its minima in October in the following month as  
335 the D215 deepens and the maximum occurs in February. The chlorophyll biomass decreases from  
336 March and a gradual decrease in ZSS is seen till July, after which the ZSS basically flattens even  
337 though the chlorophyll increases.

338 At the northernmost site of EAS i.e, off Okha, a noticeable feature is a much higher oxygen in  
339 upper ocean. The biomass above z200 is much weaker ([Fig. 4 a1](#)) compared to Mumbai as seen in  
340 the zooplankton biomass climatology which leads to a relatively lower ZSS ([Fig. 4 a2](#)). The D200  
341 shallows from February (coinciding with ZSS maximum) to its minimum in August, remains visibly  
342 flat till September and then increases steadily till December and rapidly afterwards. There's two  
343 chlorophyll peak off Okha; one in February [[Keerthi et al., 2017](#)] and the other during August in  
344 summer monsoon [[Lévy et al., 2007](#)]. The ZSS remains flat in summer monsoon period i.e, June  
345 to September, although the chlorophyll biomass increases in this time. Afterwards, ZSS gradually  
346 increases and attains its maximum in February same as the chlorophyll biomass. The ZSS sustains  
347 this maximum till March, declines rapidly in April and then gradually till July.

348 **3.4 Comparison to previous result**

349 A comparison with the zooplankton biomass and standing stock climatology of previous work  
350 [Aparna et al., 2022] is made in this section for the locations of Mumbai, Goa and Kollam. In the  
351 previous study data from 2012 to 2020 is used, while the present study includes data from 2017 to  
352 2023.

353 It is observed that D215 is shallower at all locations and as a result a lower ZSS is seen in the  
354 climatology of the present study ([Fig. 5](#)). The difference in D215 is prominent off Goa; while in the  
355 previous climatology ([Fig. 5 b1](#)) the D215 is deeper and lies along D23, in the present climatological  
356 data ([Fig. 5 b2](#)) the D215 is shallower and lies ~ 20 - 40 m above the D23 during January to April.

357 A relatively lower biomass is present above z215 year round which reflects in overall lower ZSS. This  
358 goes same for the biomass off Mumbai ([Fig. 5 a1 & a2](#)) i.e, a comparatively shallow D215 and lower  
359 ZSS in comparison with [Aparna et al., 2022]. Instead of a ZSS maxima in February, in the present  
360 data, the maxima is sustained in march, which could be due to the lower value of ZSS in February.

361 The second maxima occurs in August ([Fig. 5 d1](#)) which is less pronounced in present study ([Fig. 5](#)  
362 d2). Similar to Goa, there is dramatic decrease in the minima that occurs in October and ZSS  
363 increases rapidly post October till February. Off Kollam, a higher biomass is observed from May to  
364 June in previous study, while in the present study, along with May to June, a higher biomass is seen  
365 from September to November([Fig. 4 c2](#)) which is reflected as a minima of ZSS occurring in August  
366 ([Fig. 4 d2](#)). The higher ZSS on either side to this minima is less pronounced in previous data. This  
367 difference in ZSS is clearly seen in the correlation, which is 0.60 off Kollam, while it is 0.94 and 0.98  
368 off Mumbai and Goa, respectively. Note that the correlation only shows how similar the ZSS trend  
369 is and doesn't tell us about the deviation in magnitude in present study. Chlorophyll biomass shows  
370 stronger peak for all locations in August in present study, when the zooplankton-phytoplankton

<sup>371</sup> relationship discrepancy is observed off Kollam similar to results reported in previous climatology.

## <sup>372</sup> 4 The seasonal cycle

<sup>373</sup> In the following section we will delineate the seasonal variation of zooplankton biomass and standing  
<sup>374</sup> stock.

### <sup>375</sup> 4.1 Seasonal cycle of biomass

<sup>376</sup> Biomass contour to demarcate upper (high biomass) to lower (low biomass) regimes is devised for  
<sup>377</sup> each zooplankton time series to show their seasonality. A preliminary analysis of the biomass time  
<sup>378</sup> series in daily and monthly averaged scale shows that the biomass decreases with increasing depth  
<sup>379</sup> ([Fig. 3](#)) at all the seven locations. The rate of biomass decrease with depth, roughly defined as  
<sup>380</sup> the difference between the mean biomass at 40 m and 104 m depth, is highest off Jaigarh and  
<sup>381</sup> Mumbai as it has higher biomass in upper ocean ([Fig. 3 c2,b2](#)). This is followed by CEAS locations  
<sup>382</sup> Goa and Udupi ([Fig. 3 d2,e2](#)). While the rate of biomass decrease is lower off Kollam for 2017  
<sup>383</sup> to 2020, it becomes considerably high from thereon ([Fig. 3 f2](#)). The rate of decrease is lowest  
<sup>384</sup> off Kanyakumari. Following is the order of their decrease rate of biomass: Jaigarh ( $96 \text{ mg m}^{-3}$ ),  
<sup>385</sup> Mumbai ( $91 \text{ mg m}^{-3}$ ), Okha ( $79 \text{ mg m}^{-3}$ ), Udupi ( $78 \text{ mg m}^{-3}$ ), Kollam( $73 \text{ mg m}^{-3}$ ), Goa ( $72$   
<sup>386</sup>  $\text{mg m}^{-3}$ ) and Kanyakumari ( $39 \text{ mg m}^{-3}$ ). The mean and standard deviation is shown in [Table 3](#).  
<sup>387</sup> Following poleward along the slope, the mean biomass at 40 m off Kanyakumari is the least  $\sim$   
<sup>388</sup>  $207 \text{ mg m}^{-3}$  which increases drastically to  $272 \text{ mg m}^{-3}$  off Kollam. It decreases till Goa and  
<sup>389</sup> then increases to a maximum of  $278 \text{ mg m}^{-3}$  off Jaigarh. Off Mumbai the mean biomass is  $272$   
<sup>390</sup>  $\text{mg m}^{-3}$ , and further north off Okha, it declines to  $230 \text{ mg m}^{-3}$ . A similar trend is observed  
<sup>391</sup> in mean biomass at 104 m depth of all locations and their corresponding standard deviation. A

392 pattern that develops from this is observed, with lower mean biomass off Okha (northernmost of  
393 EAS) and off Goa (CEAS) bifurcated by higher mean biomass off Mumbai & Jaigarh; while the  
394 lower mean biomass off Udupi (CEAS) and off Kanyakumari (Southernmost of EAS) is divided by  
395 higher mean biomass off Kollam. Similarly from standard deviation of biomass it is inferred that  
396 the sites with higher biomass tends to have higher variation over time as in the case of Kollam,  
397 Jaigarh and Mumbai.

398 A comparatively weaker decline in zooplankton biomass with respect to depth off Okha ([Fig. 3](#)  
399 a1,a2) at NEAS is agreeing with earlier reported data [Madhupratap et al. \[2001\]](#), [Smith and Mad-](#)  
400 [hupratap \[2005\]](#), [Wishner et al. \[1998\]](#) where oxygen deficit at is thought to be the cause, especially  
401 during summer monsoon. The sites at SEAS, especially off Kanyakumari and 2017 to 2020 off  
402 Kollam also have weaker decrease [[Madhupratap et al., 2001](#), [Aparna et al., 2022](#)]. However, post  
403 2020 the decline in biomass with depth off Kollam is similar to that off Mumbai in stark contrast  
404 to its previous years. This is due to a strong bloom in these years. This high growth led to increase  
405 in biomass in the entire water column([Fig. 3 f1,f2](#)) and deepening of D215.

406 Analysis of the demarcating biomass contours (z175, z200, z215 of respective locations) shows  
407 strong seasonality at NEAS, CEAS and SEAS (excluding Kanyakumari). Although a shallow and  
408 seasonally invariant D215 (D175) is seen for Goa and Kollam during January 2019 to December  
409 2020. While the z175 (z215,z200) is deeper in winter monsoon throughout EAS, we see that at the  
410 NEAS regime, the upper ocean shows considerably high biomass during this period as in the case  
411 of Okha, Mumbai and Jaigarh. On the contrary at SEAS regime, the upper ocean shows higher  
412 biomass during summer monsoon as seen off Udupi, Kollam and Kanyakumari even though the  
413 z200 (z215, z175) is shallower in this period.

<sup>414</sup> **4.2 Seasonal cycle of standing stock**

415 **References**

- 416 Anna-Karin Almén and Tobias Tamlander. Temperature-related timing of the spring bloom and match between  
417 phytoplankton and zooplankton. *Marine Biology Research*, 16(8-9):674–682, 2020.
- 418 P Amol, D Shankar, V Fernando, A Mukherjee, SG Aparna, R Fernandes, GS Michael, ST Khalap, NP Satelkar,  
419 Y Agarvadekar, et al. Observed intraseasonal and seasonal variability of the west india coastal current on the  
420 continental slope. *Journal of Earth System Science*, 123(5):1045–1074, 2014.
- 421 P Amol, Suchandan Bemal, D Shankar, V Jain, V Thushara, V Vijith, and PN Vinayachandran. Modulation of  
422 chlorophyll concentration by downwelling rossby waves during the winter monsoon in the southeastern arabian  
423 sea. *Progress in Oceanography*, 186:102365, 2020.
- 424 SG Aparna, DV Desai, D Shankar, AC Anil, Shrikant Dora, and R Khedekar. Seasonal cycle of zooplankton standing  
425 stock inferred from adcp backscatter measurements in the eastern arabian sea. *Progress in Oceanography*, 203:  
426 102766, 2022.
- 427 Carin J Ashjian, Sharon L Smith, Charles N Flagg, and Nasseer Idrisi. Distribution, annual cycle, and vertical  
428 migration of acoustically derived biomass in the arabian sea during 1994–1995. *Deep Sea Research Part II:*  
429 *Topical Studies in Oceanography*, 49(12):2377–2402, 2002.
- 430 K Banse and DC English. Geographical differences in seasonality of czcs-derived phytoplankton pigment in the  
431 arabian sea for 1978–1986. *Deep Sea Research Part II: Topical Studies in Oceanography*, 47(7-8):1623–1677, 2000.
- 432 Karl Banse. Hydrography of the arabian sea shelf of india and pakistan and effects on demersal fishes. In *Deep sea*  
433 *research and oceanographic Abstracts*, volume 15, pages 45–79. Elsevier, 1968.
- 434 Karl Banse. Zooplankton: pivotal role in the control of ocean production: I. biomass and production. *ICES Journal*  
435 *of marine Science*, 52(3-4):265–277, 1995.
- 436 WE Barraclough, RJ LeBrasseur, and OD Kennedy. Shallow scattering layer in the subarctic pacific ocean: detection  
437 by high-frequency echo sounder. *Science*, 166(3905):611–613, 1969.
- 438 H. P. Batchelder, J. R. VanKeuren, R. D. Vaillancourt, and E. Swift. Spatial and temporal distributions of acoustically  
439 estimated zooplankton biomass near the marine light-mixed layers station (59°30'n, 21°00'w) in the north atlantic  
440 in may 1991. *Journal of Geophysical Research: Oceans*, 100:6549–6563, 1995. doi: 10.1029/94jc00981.
- 441 John C Brock and Charles R McClain. Interannual variability in phytoplankton blooms observed in the northwestern  
442 arabian sea during the southwest monsoon. *Journal of Geophysical Research: Oceans*, 97(C1):733–750, 1992.
- 443 John C Brock, Charles R McClain, Mark E Luther, and William W Hay. The phytoplankton bloom in the north-  
444 western arabian sea during the southwest monsoon of 1979. *Journal of Geophysical Research: Oceans*, 96(C11):  
445 20623–20642, 1991.

- 446 Abhisek Chatterjee, D Shankar, SSC Shenoi, GV Reddy, GS Michael, M Ravichandran, VV Gopalkrishna,  
447 EP Rama Rao, TVS Udaya Bhaskar, and VN Sanjeevan. A new atlas of temperature and salinity for the north  
448 indian ocean. *Journal of Earth System Science*, 121:559–593, 2012.
- 449 Anya Chaudhuri, D Shankar, SG Aparna, P Amol, V Fernando, A Kankonkar, GS Michael, NP Satelkar, ST Khalap,  
450 AP Tari, et al. Observed variability of the west india coastal current on the continental slope from 2009–2018.  
451 *Journal of Earth System Science*, 129(1):57, 2020.
- 452 Anya Chaudhuri, P Amol, D Shankar, S Mukhopadhyay, SG Aparna, V Fernando, and A Kankonkar. Observed  
453 variability of the west india coastal current on the continental shelf from 2010–2017. *Journal of Earth System  
454 Science*, 130:1–21, 2021.
- 455 Boris Cisewski, Volker H Strass, Monika Rhein, and Sören Krägesky. Seasonal variation of diel vertical migration  
456 of zooplankton from adcp backscatter time series data in the lazarev sea, antarctica. *Deep Sea Research Part I:  
457 Oceanographic Research Papers*, 57(1):78–94, 2010.
- 458 Kent L Deines. Backscatter estimation using broadband acoustic doppler current profilers. In *Proceedings of the  
459 IEEE Sixth Working Conference on Current Measurement (Cat. No. 99CH36331)*, pages 249–253. IEEE, 1999.
- 460 A Edvardsen, D Slagstad, KS Tande, and P Jaccard. Assessing zooplankton advection in the barents sea using  
461 underway measurements and modelling. *Fisheries Oceanography*, 12(2):61–74, 2003.
- 462 S Fielding, G Griffiths, and HSJ Roe. The biological validation of adcp acoustic backscatter through direct comparison  
463 with net samples and model predictions based on acoustic-scattering models. *ICES Journal of Marine Science*,  
464 61(2):184–200, 2004.
- 465 Charles N Flagg and Sharon L Smith. On the use of the acoustic doppler current profiler to measure zooplankton  
466 abundance. *Deep Sea Research Part A. Oceanographic Research Papers*, 36(3):455–474, 1989.
- 467 H. E. García, R. A. Locarnini, T. P. Boyer, J. I. Antonov, A. V. Mishonov, O. K. Baranova, M. M. Zweng, J. R.  
468 Reagan, and D. R. Johnson. Dissolved oxygen, apparent oxygen utilization, and oxygen saturation. *NOAA Atlas  
469 NESDIS 75*, 3, 2014.
- 470 Charles H Greene, Peter H Wiebe, Chris Pelkie, Mark C Benfield, and Jacqueline M Popp. Three-dimensional  
471 acoustic visualization of zooplankton patchiness. *Deep Sea Research Part II: Topical Studies in Oceanography*, 45  
472 (7):1201–1217, 1998.
- 473 Charles F Greenlaw. Acoustical estimation of zooplankton populations 1. *Limnology and Oceanography*, 24(2):  
474 226–242, 1979.
- 475 Davide Guerra, Katrin Schroeder, Mireno Borghini, Elisa Camatti, Marco Pansera, Anna Schroeder, Stefania  
476 Sparnocchia, and Jacopo Chiggiato. Zooplankton diel vertical migration in the corsica channel (north-western  
477 mediterranean sea) detected by a moored acoustic doppler current profiler. *Ocean Science*, 15(3):631–649, 2019.

- 478 Graeme C Hays. A review of the adaptive significance and ecosystem consequences of zooplankton diel vertical  
479 migrations. In *Migrations and Dispersal of Marine Organisms: Proceedings of the 37 th European Marine Biology*  
480 *Symposium held in Reykjavik, Iceland, 5–9 August 2002*, pages 163–170. Springer, 2003.
- 481 PJ Herring, MJR Fasham, AR Weeks, JCP Hemmings, HSJ Roe, PR Pugh, S Holley, NA Crisp, and MV Angel.  
482 Across-slope relations between the biological populations, the euphotic zone and the oxygen minimum layer off  
483 the coast of oman during the southwest monsoon (august, 1994). *Progress in Oceanography*, 41(1):69–109, 1998.
- 484 Karen J Heywood, S Scrope-Howe, and ED Barton. Estimation of zooplankton abundance from shipborne adcp  
485 backscatter. *Deep Sea Research Part A. Oceanographic Research Papers*, 38(6):677–691, 1991.
- 486 Laura Hobbs, Neil S Banas, Jonathan H Cohen, Finlo R Cottier, Jørgen Berge, and Øystein Varpe. A marine  
487 zooplankton community vertically structured by light across diel to interannual timescales. *Biology Letters*, 17(2):  
488 20200810, 2021.
- 489 Raleigh R Hood, Lynnath E Beckley, and Jerry D Wiggert. Biogeochemical and ecological impacts of boundary  
490 currents in the indian ocean. *Progress in Oceanography*, 156:290–325, 2017.
- 491 Ryuichiro Inoue, Minoru Kitamura, and Tetsuichi Fujiki. Diel vertical migration of zooplankton at the s 1 biogeo-  
492 chemical mooring revealed from acoustic backscattering strength. *Journal of Geophysical Research: Oceans*, 121  
493 (2):1031–1050, 2016.
- 494 Songnian Jiang, Tommy D Dickey, Deborah K Steinberg, and Laurence P Madin. Temporal variability of zooplankton  
495 biomass from adcp backscatter time series data at the bermuda testbed mooring site. *Deep Sea Research Part I:*  
496 *Oceanographic Research Papers*, 54(4):608–636, 2007.
- 497 R Jyothibabu, NV Madhu, H Habeebrehman, KV Jayalakshmy, KKC Nair, and CT Achuthankutty. Re-evaluation  
498 of ‘paradox of mesozooplankton’ in the eastern arabian sea based on ship and satellite observations. *Journal of*  
499 *Marine Systems*, 81(3):235–251, 2010.
- 500 Myounghee Kang, Sunyoung Oh, Wooseok Oh, Dong-Jin Kang, SungHyun Nam, and Kyounghoon Lee. Acoustic  
501 characterization of fish and macroplankton communities in the seychelles-chagos thermocline ridge of the southwest  
502 indian ocean. *Deep Sea Research Part II: Topical Studies in Oceanography*, 213:105356, 2024.
- 503 Madhavan Girijakumari Keerthi, Matthieu Lengaigne, Marina Levy, Jerome Vialard, Vallivattathillam Parvathi,  
504 Clément de Boyer Montégut, Christian Ethé, Olivier Aumont, Iyyappan Suresh, Valiya Parambil Akhil, et al.  
505 Physical control of interannual variations of the winter chlorophyll bloom in the northern arabian sea. *Biogeosciences*, 14(15):3615–3632, 2017.
- 507 Corinne Le Qu, Robbie M Andrew, Josep G Canadell, Stephen Sitch, Jan Ivar Korsbakken, Glen P Peters, Andrew C  
508 Manning, Thomas A Boden, Pieter P Tans, Richard A Houghton, et al. Global carbon budget 2016. *Earth System*  
509 *Science Data*, 8(2):605–649, 2016.

- 510 Marina Lévy, D Shankar, J-M André, SSC Shenoi, Fabien Durand, and Clément de Boyer Montégut. Basin-wide  
511 seasonal evolution of the indian ocean's phytoplankton blooms. *Journal of Geophysical Research: Oceans*, 112  
512 (C12), 2007.
- 513 M Li, A Gargett, and K Denman. What determines seasonal and interannual variability of phytoplankton and  
514 zooplankton in strongly estuarine systems? *Estuarine, Coastal and Shelf Science*, 50(4):467–488, 2000.
- 515 Yanliang Liu, Jingsong Guo, Yuhuan Xue, Chalermrat Sangmanee, Huiwu Wang, Chang Zhao, Somkiat Khokiat-  
516 tiwong, and Weidong Yu. Seasonal variation in diel vertical migration of zooplankton and micronekton in the  
517 andaman sea observed by a moored adcp. *Deep Sea Research Part I: Oceanographic Research Papers*, 179:103663,  
518 2022.
- 519 M Madhupratap, P Haridas, Neelam Ramaiah, and CT Achuthankutty. Zooplankton of the southwest coast of india:  
520 abundance, composition, temporal and spatial variability in 1987. 1992.
- 521 M Madhupratap, TC Gopalakrishnan, P Haridas, KKC Nair, PN Aravindakshan, G Padmavati, and Shiney Paul.  
522 Lack of seasonal and geographic variation in mesozooplankton biomass in the arabian sea and its structure in the  
523 mixed layer. *Current science. Bangalore*, 71(11):863–868, 1996a.
- 524 M Madhupratap, S Prasanna Kumar, PMA Bhattachari, M Dileep Kumar, S Raghukumar, KKC Nair, and N Rama-  
525 iah. Mechanism of the biological response to winter cooling in the northeastern arabian sea. *Nature*, 384(6609):  
526 549–552, 1996b.
- 527 M Madhupratap, TC Gopalakrishnan, P Haridas, and KKC Nair. Mesozooplankton biomass, composition and  
528 distribution in the arabian sea during the fall intermonsoon: implications of oxygen gradients. *Deep Sea Research  
529 Part II: Topical Studies in Oceanography*, 48(6-7):1345–1368, 2001.
- 530 PA Maheswaran, G Rajesh, C Revichandran, and KKC Nair. Upwelling and associated hydrography along the west  
531 coast of india during southwest monsoon, 1999. 2000.
- 532 JP McCreary, Raghu Murtugudde, Jerome Vialard, PN Vinayachandran, Jerry D Wiggert, Raleigh R Hood,  
533 D Shankar, and S Shetye. Biophysical processes in the indian ocean. *Indian Ocean biogeochemical processes  
534 and ecological variability*, 185:9–32, 2009.
- 535 Julian P McCreary Jr, Pijush K Kundu, and Robert L Molinari. A numerical investigation of dynamics, thermody-  
536 namics and mixed-layer processes in the indian ocean. *Progress in Oceanography*, 31(3):181–244, 1993.
- 537 Donald C McNaught. Acoustical determination of zooplankton distribution. In *Proc. 11th Conf. Great lakes Res.*,  
538 pages 76–84, 1968.
- 539 A Mukherjee, D Shankar, V Fernando, P Amol, SG Aparna, R Fernandes, GS Michael, ST Khalap, NP Satelkar,  
540 Y Agarvadekar, et al. Observed seasonal and intraseasonal variability of the east india coastal current on the  
541 continental slope. *Journal of Earth System Science*, 123(6):1197–1232, 2014.

- 542 S Mukhopadhyay, D Shankar, SG Aparna, A Mukherjee, V Fernando, A Kankonkar, S Khalap, NP Satelkar,  
543 MG Gaonkar, AP Tari, et al. Observed variability of the east india coastal current on the continental slope  
544 during 2009–2018. *Journal of Earth System Science*, 129:1–22, 2020.
- 545 Jerry Mullison. Backscatter estimation using broadband acoustic doppler current profilers-updated. In *Proceedings*  
546 *of the ASCE Hydraulic Measurements & Experimental Methods Conference, Durham, NH, USA*, pages 9–12,  
547 2017.
- 548 KKC Nair, M Madhupratap, TC Gopalakrishnan, P Haridas, and Mangesh Gauns. The arabian sea: physical  
549 environment, zooplankton and myctophid abundance. 1999.
- 550 PV Nair. Primary productivity in the indian seas. *CMFRI Bulletin*, 22:1–63, 1970.
- 551 Lingyun Nie, Jianchao Li, Hao Wu, Wenchao Zhang, Yongjun Tian, Yang Liu, Peng Sun, Zhenjiang Ye, Shuyang  
552 Ma, and Qinfeng Gao. The influence of ocean processes on fine-scale changes in the yellow sea cold water mass  
553 boundary area structure based on acoustic observations. *Remote Sensing*, 15(17):4272, 2023.
- 554 MD Ohman and H-J Hirche. Density-dependent mortality in an oceanic copepod population. *Nature*, 412(6847):  
555 638–641, 2001.
- 556 G Padmavati, P Haridas, KKC Nair, TC Gopalakrishnan, P Shiney, and M Madhupratap. Vertical distribution of  
557 mesozooplankton in the central and eastern arabian sea during the winter monsoon. *Journal of Plankton Research*,  
558 20(2):343–354, 1998.
- 559 MR Patil, CP Ramamirtham, P Udaya Varma, and CP Nair. Hydrography of the west coast of india during the  
560 pre-monsoon period of the year 1962. *Journal of marine biological association of India*, 6(1):151–164, 1964.
- 561 Richard Edward Pieper. *A study of the relationship between zooplankton and high-frequency scattering of underwater*  
562 *sound*. PhD thesis, University of British Columbia, 1971.
- 563 SA Piontковски, R Williams, and TA Melnik. Spatial heterogeneity, biomass and size structure of plankton of the  
564 indian ocean: some general trends. *Marine ecology progress series*, pages 219–227, 1995.
- 565 Emmanuel Potiris, Constantin Frangoulis, Alkiviadis Kalampokis, Manolis Ntoumas, Manos Pettas, George Peti-  
566 hakis, and Vassilis Zervakis. Acoustic doppler current profiler observations of migration patterns of zooplankton  
567 in the cretan sea. *Ocean Science*, 14(4):783–800, 2018.
- 568 SZ Qasim. Biological productivity of the indian ocean. 1977.
- 569 CP Ramamirtham and AVS Murty. Hydrography of the west coast of india during the pre-monsoon period of the  
570 year 1962—part 2: in and offshore waters of the konkan and malabar coasts. *Journal of the Marine Biological*  
571 *Association of India*, 7(1):150–168, 1965.
- 572 S Ramamurthy. Studies on the plankton of the north kanara coast in relation to the pelagic fishery. *Journal of*  
573 *Marine Biological Association of India*, 7(1):127–149, 1965.

- 574 Mehbuba Rehim and Mudassar Imran. Dynamical analysis of a delay model of phytoplankton–zooplankton interac-  
575 tion. *Applied Mathematical Modelling*, 36(2):638–647, 2012.
- 576 T. P. Rippeth and J. H. Simpson. Diurnal signals in vertical motions on the hebridean shelf. *Limnology and*  
577 *Oceanography*, 43:1690–1696, 1998. doi: 10.4319/lo.1998.43.7.1690.
- 578 John H Ryther, John R Hall, Allan K Pease, Andrew Bakun, and Mark M Jones. Primary organic production in  
579 relation to the chemistry and hydrography of the western indian ocean 1. *Limnology and Oceanography*, 11(3):  
580 371–380, 1966.
- 581 D Sameoto and S Paulowich. The use of 120 khz sonar in zooplankton studies. In *OCEANS'77 Conference Record*,  
582 pages 523–528. IEEE, 1977.
- 583 D Shankar and SR Shetye. On the dynamics of the lakshadweep high and low in the southeastern arabian sea.  
584 *Journal of Geophysical Research: Oceans*, 102(C6):12551–12562, 1997.
- 585 D Shankar, R Remya, PN Vinayachandran, Abhisek Chatterjee, and Ambica Behera. Inhibition of mixed-layer  
586 deepening during winter in the northeastern arabian sea by the west india coastal current. *Climate Dynamics*,  
587 47:1049–1072, 2016.
- 588 D Shankar, R Remya, AC Anil, and V Vijith. Role of physical processes in determining the nature of fisheries in the  
589 eastern arabian sea. *Progress in Oceanography*, 172:124–158, 2019.
- 590 SR Shetye and AD Gouveia. Coastal circulation in the north indian ocean: Coastal segment (14, sw). John Wiley  
591 and Sons, New York, USA, 1998.
- 592 SR Shetye, AD Gouveia, SSC Shenoi, D Sundar, GS Michael, AM Almeida, and K Santanam. Hydrography and  
593 circulation off the west coast of india during the southwest monsoon 1987. 1990.
- 594 SR Shetye, AD Gouveia, SSC Shenoi, GS Michael, D Sundar, AM Almeida, and K Santanam. The coastal current  
595 off western india during the northeast monsoon. *Deep Sea Research Part A. Oceanographic Research Papers*, 38  
596 (12):1517–1529, 1991.
- 597 SR Shetye, AD Gouveia, and SSC Shenoi. Does winter cooling lead to the subsurface salinity minimum off saurashtra,  
598 india? *Oceanography of the Indian Ocean*, pages 617–625, 1992.
- 599 Greg M Silsbe, Michael J Behrenfeld, Kimberly H Halsey, Allen J Milligan, and Toby K Westberry. The cafe model:  
600 A net production model for global ocean phytoplankton. *Global Biogeochemical Cycles*, 30(12):1756–1777, 2016.
- 601 Houssem Smeti, Marc Pagano, Christophe Menkes, Anne Lebourges-Dhaussy, Brian PV Hunt, Valerie Allain, Martine  
602 Rodier, Florian De Boissieu, Elodie Kestenare, and Cherif Sammari. Spatial and temporal variability of zooplank-  
603 ton off n ew c alifornia (s outhwestern p acific) from acoustics and net measurements. *Journal of Geophysical*  
604 *Research: Oceans*, 120(4):2676–2700, 2015.

- 605 SL Smith and M Madhupratap. Mesozooplankton of the arabian sea: patterns influenced by seasons, upwelling, and  
606 oxygen concentrations. *Progress in Oceanography*, 65(2-4):214–239, 2005.
- 607 Patnaik Sreenivas, KVKRK Patnaik, and KVSR Prasad. Monthly variability of mixed layer over arabian sea using  
608 argo data. *Marine Geodesy*, 31(1):17–38, 2008.
- 609 R Subrahmanyam. Studies on the phytoplankton of the west coast of india: Part ii. physical and chemical factors  
610 influencing the production of phytoplankton, with remarks on the cycle of nutrients and on the relationship of  
611 the phosphate-content to fish landings. In *Proceedings/Indian Academy of Sciences*, volume 50, pages 189–252.  
612 Springer, 1959.
- 613 R Subrahmanyam and AH Sarma. Studies on the phytoplankton of the west coast of india. part iii. seasonal variation  
614 of the phytoplankters and environmental factors. *Indian Journal of Fisheries*, 7(2):307–336, 1960.
- 615 Laura Ursella, Vanessa Cardin, Mirna Batistić, Rade Garić, and Miroslav Gačić. Evidence of zooplankton vertical  
616 migration from continuous southern adriatic buoy current-meter records. *Progress in oceanography*, 167:78–96,  
617 2018.
- 618 Laura Ursella, Sara Pensieri, Enric Pallàs-Sanz, Sharon Z Herzka, Roberto Bozzano, Miguel Tenreiro, Vanessa Cardin,  
619 Julio Candela, and Julio Sheinbaum. Diel, lunar and seasonal vertical migration in the deep western gulf of mexico  
620 evidenced from a long-term data series of acoustic backscatter. *Progress in Oceanography*, 195:102562, 2021.
- 621 V Vijith, PN Vinayachandran, V Thushara, P Amol, D Shankar, and AC Anil. Consequences of inhibition of mixed-  
622 layer deepening by the west india coastal current for winter phytoplankton bloom in the northeastern arabian sea.  
623 *Journal of Geophysical Research: Oceans*, 121(9):6583–6603, 2016.
- 624 Peter H Wiebe, Charles H Greene, Timothy K Stanton, and Janusz Burczynski. Sound scattering by live zooplankton  
625 and micronekton: empirical studies with a dual-beam acoustical system. *The Journal of the Acoustical Society of  
626 America*, 88(5):2346–2360, 1990.
- 627 Monika Winder and Daniel E Schindler. Climatic effects on the phenology of lake processes. *Global change biology*,  
628 10(11):1844–1856, 2004.
- 629 Karen F Wishner, Marcia M Gowing, and Celia Gelfman. Mesozooplankton biomass in the upper 1000 m in the  
630 arabian sea: overall seasonal and geographic patterns, and relationship to oxygen gradients. *Deep Sea Research  
631 Part II: Topical Studies in Oceanography*, 45(10-11):2405–2432, 1998.

Table 1: ADCP deployment details at the locations. The temporal resolution is 1 hour, bin size(vertical resolution) 4 m. All ADCPs are operated at 153.3 kHz. The moorings are at a water column depth of 950 - 1200 m on the continental slope and are serviced on yearly basis according to ship availability. The 6th column consists of Reference echo intensity (Er) for each beam, while the 7th column contains the corresponding RSSI conversion factor [Deines, 1999].

Station (Position; $^{\circ}$ E, $^{\circ}$ N)	Date		Depth			
	Deployment	Recovery	Ocean	ADCP	Er	Kc
Okha (67.47, 22.26)	01/10/2018	01/12/2019	996	118	37 , 37 , 37 , 36	0.42 , 0.44 , 0.42 , 0.43
	01/12/2019	04/12/2020	1166	312	39 , 36 , 38 , 36	0.42 , 0.44 , 0.42 , 0.43
	04/12/2020	08/03/2022	1021	144	41 , 37 , 38 , 37	0.42 , 0.44 , 0.42 , 0.43
	08/03/2022	01/01/2023	1019	142	37 , 38 , 39 , 36	0.42 , 0.44 , 0.42 , 0.43
Mumbai (69.24, 20.01)	09/11/2017	29/09/2018	1025	150	36 , 34 , 39 , 42	0.40 , 0.40 , 0.40 , 0.40
	29/09/2018	29/11/2019	1122	125	35 , 36 , 39 , 42	0.40 , 0.40 , 0.40 , 0.40
	29/11/2019	02/12/2020	1143	164	37 , 34 , 39 , 43	0.40 , 0.40 , 0.40 , 0.40
	02/12/2020	06/03/2022	1125	142	36 , 34 , 39 , 42	0.40 , 0.40 , 0.40 , 0.40
	07/03/2022	02/01/2023	1103	158	37 , 34 , 40 , 43	0.40 , 0.40 , 0.40 , 0.40
Jaigarh (71.12, 17.53)	27/10/2017	27/09/2018	1039	198	32 , 35 , 33 , 32	0.45 , 0.45 , 0.45 , 0.45
	27/09/2018	30/10/2019	1032	164	32 , 35 , 33 , 31	0.45 , 0.45 , 0.45 , 0.45
	03/11/2019	30/11/2020	1142	264	32 , 36 , 33 , 32	0.45 , 0.45 , 0.45 , 0.45
	30/11/2020	05/03/2022	1099	119	33 , 36 , 34 , 32	0.45 , 0.45 , 0.45 , 0.45
Goa (72.74, 15.17)	03/10/2017	25/09/2018	1000	174	35 , 37 , 34 , 35	0.44 , 0.44 , 0.40 , 0.41
	25/09/2018	16/10/2019	969	145	38 , 36 , 36 , 34	0.44 , 0.44 , 0.40 , 0.41
	16/10/2019	29/11/2020	966	143	44 , 38 , 36 , 43	0.44 , 0.44 , 0.40 , 0.41
	29/11/2020	03/03/2022	985	157	35 , 40 , 35 , 38	0.44 , 0.44 , 0.40 , 0.41
	03/03/2022	05/01/2023	984	159	35 , 38 , 35 , 34	0.44 , 0.44 , 0.40 , 0.41
Udupi (74.04, 12.5)	05/10/2017	06/10/2018	1028	176	44 , 46 , 29 , 35	0.45 , 0.45 , 0.45 , 0.45
	06/10/2018	18/10/2019	1027	179	32 , 38 , 30 , 36	0.45 , 0.45 , 0.45 , 0.45
	18/10/2019	11/12/2020	1018	168	33 , 37 , 31 , 38	0.45 , 0.45 , 0.45 , 0.45
	11/03/2022	06/01/2023	1036	155	31 , 32 , 32 , 33	0.45 , 0.45 , 0.45 , 0.45
Kollam (75.44, 9.05)	07/10/2017	08/10/2018	1174	200	43 , 55 , 45 , 43	0.49 , 0.50 , 0.49 , 0.50
	08/10/2018	20/10/2019	1160	123	49 , 62 , 46 , 46	0.49 , 0.50 , 0.49 , 0.50
	20/10/2019	13/12/2020	1209	176	52 , 61 , 54 , 55	0.49 , 0.50 , 0.49 , 0.50
	13/12/2020	13/03/2022	1129	91	49 , 51 , 46 , 47	0.49 , 0.50 , 0.49 , 0.50
	13/03/2022	08/01/2023	1149	164	41 , 48 , 43 , 41	0.49 , 0.50 , 0.49 , 0.50
Kanyakumari (77.39, 6.96)	16/11/2016	08/10/2017	1096	252	37 , 36 , 37 , 37	0.42 , 0.44 , 0.42 , 0.43
	08/10/2017	10/10/2018	1055	181	32 , 34 , 38 , 35	0.45 , 0.45 , 0.45 , 0.45
	10/10/2018	22/10/2019	1075	180	36 , 34 , 39 , 36	0.45 , 0.45 , 0.45 , 0.45
	22/10/2019	14/12/2020	1060	167	33 , 35 , 36 , 35	0.45 , 0.45 , 0.45 , 0.45
	14/12/2020	14/03/2022	1184	287	34 , 36 , 36 , 35	0.45 , 0.45 , 0.45 , 0.45

Table 2:  
 Volumetric samples of zooplankton of various stations. The sampling depth range is standardised for later years for bin range of 0–25m, 25–50m, 50–75m, 75–100m, 100–150m. The abbreviations are in the following manner: Okha (O), Mumbai (M), Jaigarh (J), Goa (G), Udupi (U), Kollam (K), Kanyakumari (KK); The number tags corresponds to particular cruise of a station.

Sample number	Tag	Lat( $^{\circ}$ N)	Lon( $^{\circ}$ E)	Date	Time (IST)	Sampling depth range (m)
1-3	G1	15.18	72.79	25 Sep 18	452	50–25, 100–50, 150–100
4-6	G2	15.16	72.71	25 Sep 18	2108	50–25, 100–50, 150–100
7-10	G2	15.16	72.71	25 Sep 18	2137	40–20, 60–40, 80–60, 100–80
11-14	J1			26 Sep 18	2000	40–20, 60–40, 80–60, 100–80
15-17	J2			27 Sep 18	2000	50–25, 100–50, 150–100
18-21	J2			27 Sep 18	2100	40–20, 60–40, 80–60, 100–80
22-25	M1	20	69.19	28 Sep 18	2135	40–20, 60–40, 80–60, 100–80
26-27	M1	20	69.19	28 Sep 18	2205	50–25, 100–50
28-29	M2	20.01	69.2	29 Sep 18	2035	50–25, 100–50
30-33	M2	20.01	69.2	29 Sep 18	2057	40–20, 60–40, 80–60, 100–80
34-37	U1			5 Oct 18	2000	40–20, 60–40, 80–60, 100–80
38-40	U1			5 Oct 18	2100	50–25, 100–50, 150–100
41-43	U2			6 Oct 18	2000	50–25, 100–50, 150–100
44-47	U2			6 Oct 18	2100	40–20, 60–40, 80–60, 100–80
48-51	K1	9.06	75.42	8 Oct 18	421	40–20, 60–40, 80–60, 100–80
52-54	K1	9.06	75.42	8 Oct 18	449	50–25, 100–50, 150–100
55-56	K2	9.04	75.4	8 Oct 18	2027	50–25, 100–50
57-60	K2	9.04	75.4	8 Oct 18	2045	40–20, 60–40, 80–60, 100–80
61-64	G2	15.16	72.74	16 Oct 19	829	50–25, 75–50, 100–75, 150–100
65-67	G3	15.16	72.74	16 Oct 19	1812	50–25, 75–50, 100–75
68-70	K2	9.02	75.42	20 Oct 19	840	50–25, 75–50, 100–75
71-74	K3	9.04	75.43	20 Oct 19	1934	50–25, 75–50, 100–75, 150–100
75-78	KK1			22 Oct 19	742	50–25, 75–50, 100–75, 150–100
79-82	KK2			22 Oct 19	1925	50–25, 75–50, 100–75, 150–100
83-86	J1			30 Oct 19	324	50–25, 75–50, 100–75, 150–100
87-89	J2			4 Nov 19	946	75–50, 100–75, 150–100
90-92	M2	19.98	69.22	29 Nov 19	1434	50–25, 75–50, 100–75
93-96	M3	20.01	69.23	30 Nov 19	958	50–25, 75–50, 100–75, 150–100
97-100	O1	22.24	67.49	1 Dec 19	937	50–25, 75–50, 100–75, 150–100
101	O2	22.25	67.46	1 Dec 19	1957	150–100
102-105	G3	15.68	73.22	28 Nov 20	930	50–25, 75–50, 100–75, 150–100
105-108	G4	15.32	73.22	29 Nov 20	1558	50–25, 75–50, 100–75, 150–100
108-110	J2	17.85	71.21	30 Nov 20	1458	75–50, 100–75, 150–100
111-114	J3	17.91	71.21	1 Dec 20	1052	50–25, 75–50, 100–75, 150–100
115-118	M4	20.03	69.38	2 Dec 20	2016	50–25, 75–50, 100–75, 150–100
119-00	O2	22.41	67.8	4 Dec 20	953	150–100
120-123	O3	22.41	67.79	4 Dec 20	2011	50–25, 75–50, 100–75, 150–100
124-127	K3	9.11	75.72	12 Dec 20	2335	50–25, 75–50, 100–75, 150–100
128-131	K4	9.06	75.74	13 Dec 20	1507	50–25, 75–50, 100–75, 150–100
132-134	KK1	7.62	77.63	14 Dec 20	1226	50–25, 75–50
135-138	KK2	7.62	77.63	14 Dec 20	2047	50–25, 75–50, 100–75, 150–100
139-142	G4	15.32	73.21	3 Mar 22	823	50–25, 75–50, 100–75, 150–100
143-146	G5	15.68	73.21	4 Mar 22	1030	50–25, 75–50, 100–75, 150–100
147-150	M5	19.99	69.23	7 Mar 22	957	50–25, 75–50, 100–75, 150–100
151-154	O3	22.24	67.5	8 Mar 22	806	50–25, 75–50, 100–75, 150–100
155-158	U3	12.5	74.04	12 Mar 22	1156	50–25, 75–50, 100–75, 150–100
159-160	K4	9.04	75.42	13 Mar 22	1027	50–25, 75–50, 100–75
161-164	KK3	6.97	77.4	15 Mar 22	1220	50–25, 75–50, 100–75, 150–100

Table 3:

The mean, standard deviation at 40 and 104 m of biomass at 7 mooring sites and their difference is tabulated. All units are in  $mg\ m^{-3}$ .

	40 m		104 m		difference
	Mean	std	Mean	std	
Okha	230.42	22.84	151.68	25.58	78.74
Mumbai	272.86	34.95	182.24	30.34	90.62
Jaigarh	278.45	36.52	182.96	48.89	95.49
Goa	235.22	30.34	163.02	36.54	72.2
Udupi	247.81	34.37	169.37	38.8	78.43
Kollam	272.56	54.94	198.89	50.08	73.67
Kanyakumari	207.07	30.42	167.63	20.89	39.44

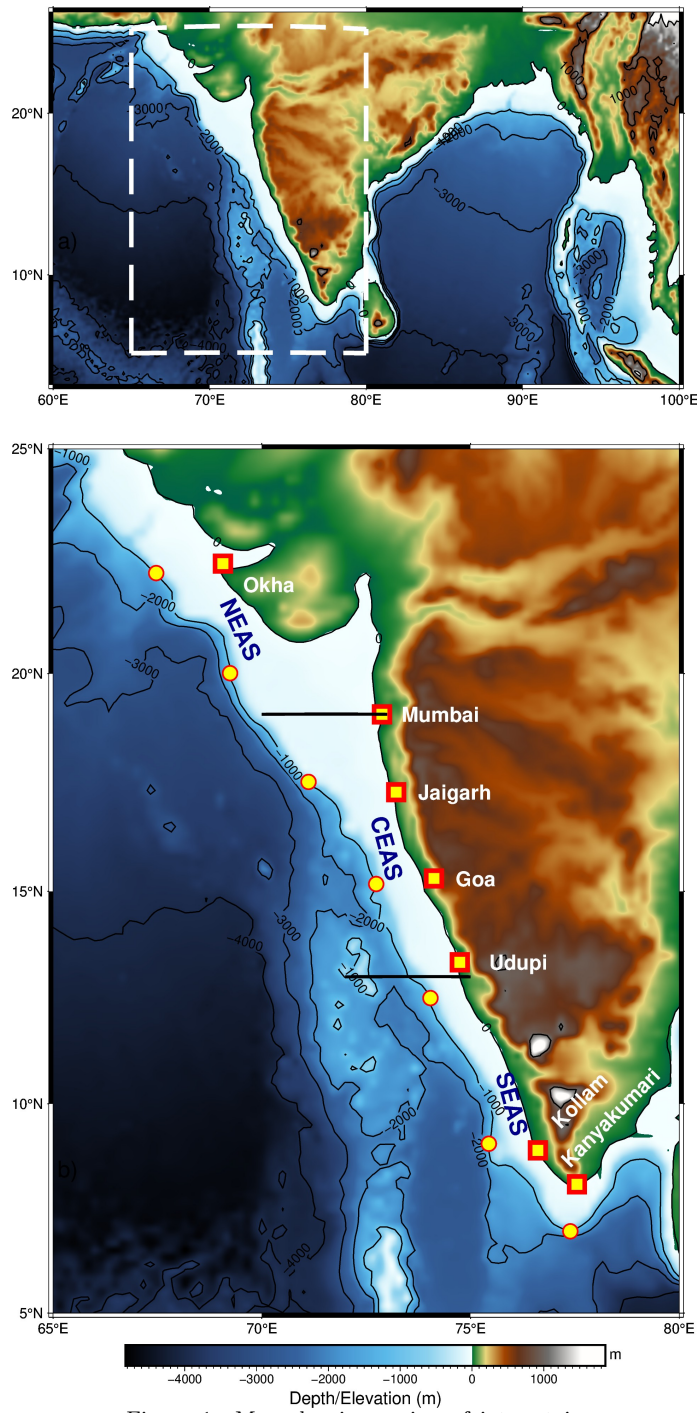


Figure 1: Map showing region of interest in eastern Arabian Sea. The slope moorings are deployed at 1000 m depth as shown in the bathymetry contour.

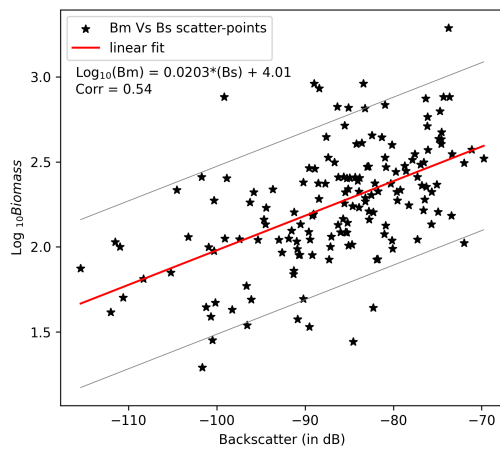


Figure 2: The linear fit line of Biomass (scale of log) and backscattering strength (in dB). The linear fit line is within the error range of previous result of [Aparna et al., 2022] onto which latest zooplankton volumetric sample data is added.

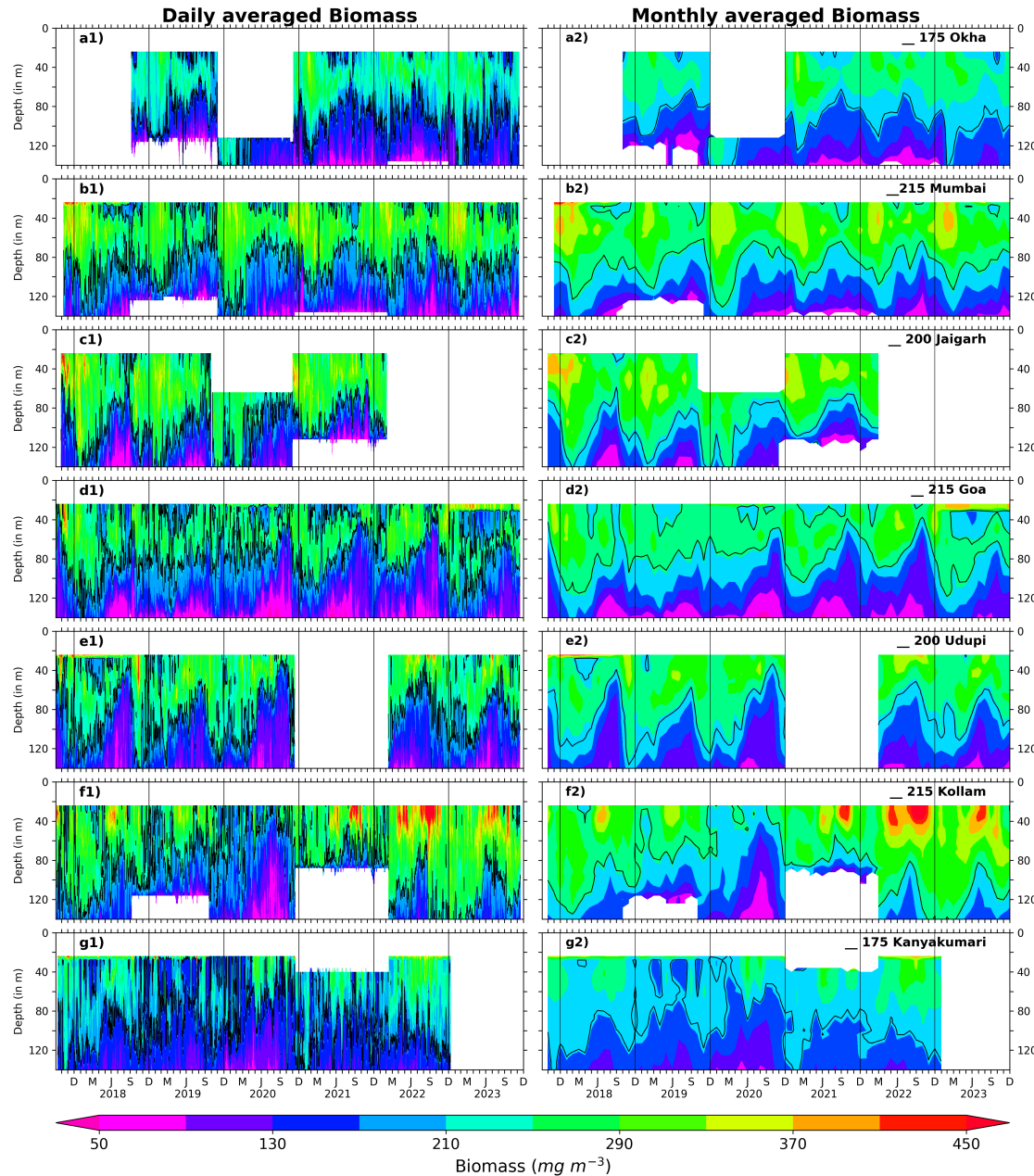


Figure 3: The Daily and monthly averaged biomass for EAS moorings, north (top) to south (bottom). The black contours are marking of  $175 \text{ mg m}^{-3}$  biomass for Okha and Kanyakumari;  $200 \text{ mg m}^{-3}$  for Jaigarh and Udupi;  $215 \text{ mg m}^{-3}$  for Mumbai, Goa and Kollam. The biomass contours are distinct and different based on the physico-chemical parameters and the one that best explains seasonality at respective location.

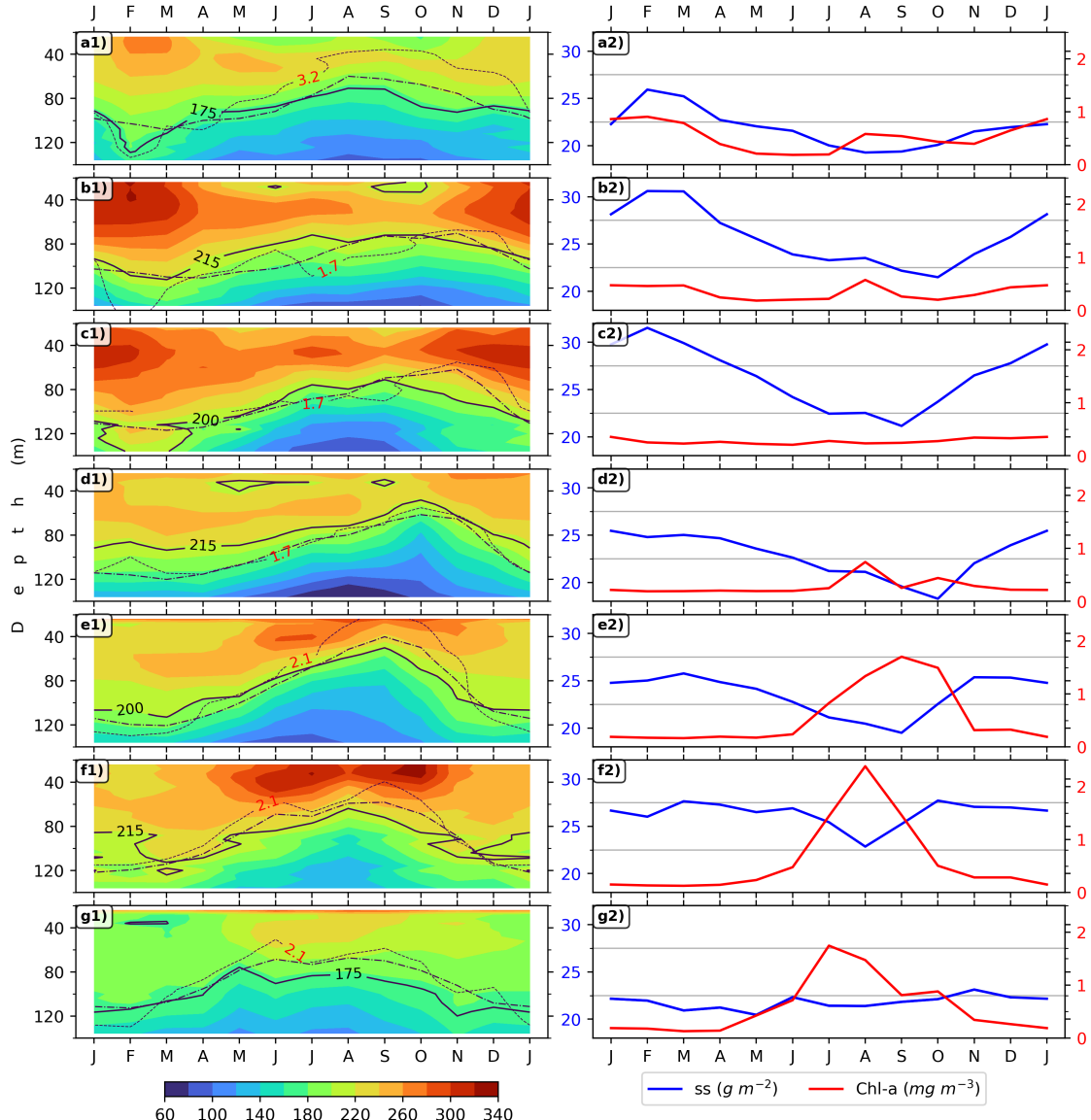


Figure 4: Monthly climatology of zooplankton biomass is shown in left panels for 7 locations, (top to bottom is southward). The D175, D200 & D215 are shown in solid lines; dashed line represents the depth of  $23^{\circ}\text{C}$  isotherm; oxygen contours are shown in dotted lines and labeled for each mooring. The plot labels are as follows: a1 & a2 for Okha, b1 & b2 for Mumbai, c1 & c2 for Jaigarh, d1 & d2 for Goa, e1 & e2 for Udupi, f1 & f2 for Kollam, g1 & g2 for Kanyakumari. The right set of panel plots is showing ZSS and chlorophyll climatology for respective locations.

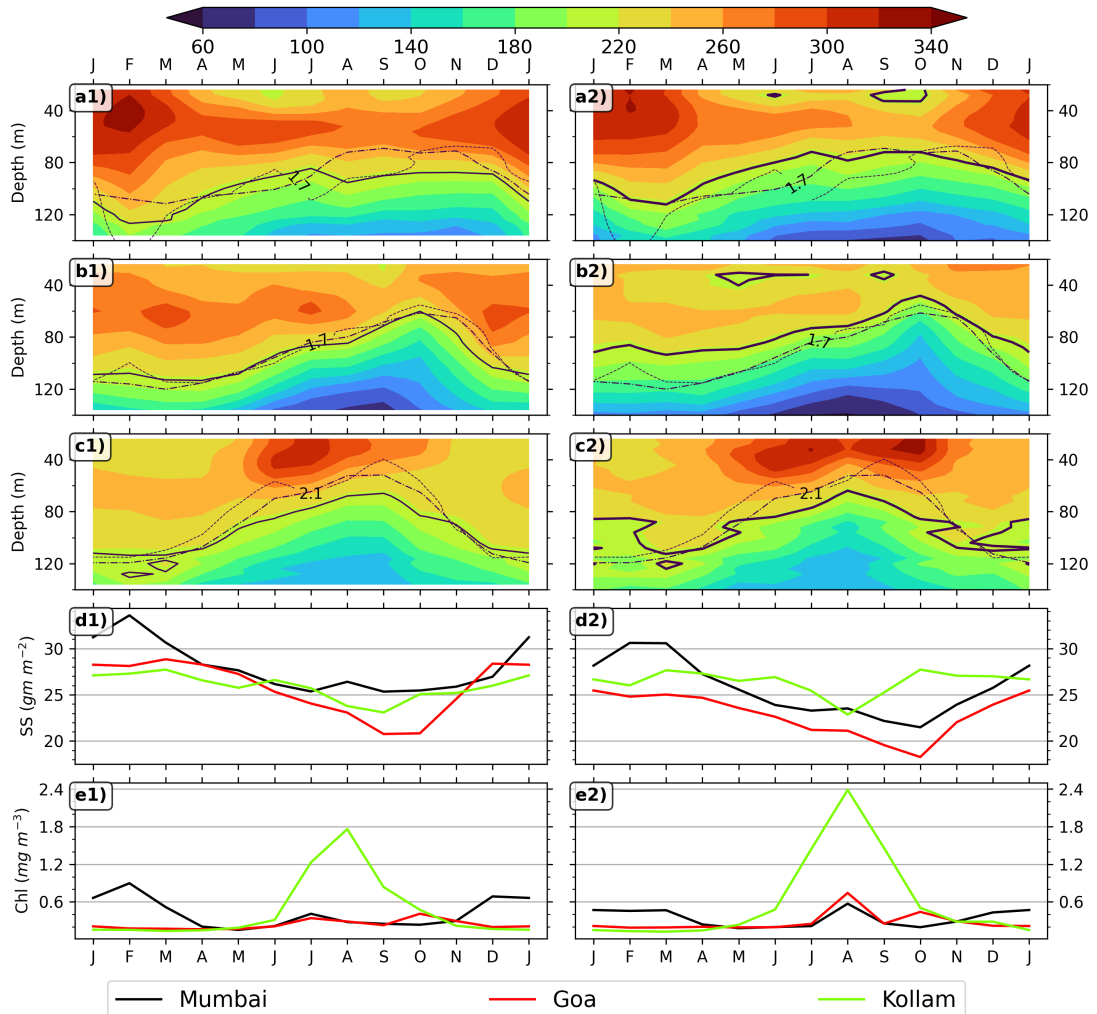


Figure 5: Monthly climatology of zooplankton biomass is shown in left panels for 3 locations which were earlier used in [Aparna et al., 2022]; a1, b1 & c1 is the biomass climatology for Mumbai, Goa and Kollam, d1 is for ZSS climatology, e1 is for chlorophyll biomass climatology; a2, b2, c2, d2 & e2 is same but based on data from 2017 to 2023. The D215 is shown in solid line. The dashed line represents the depth of 23 °C isotherm; oxygen contours are shown in dotted lines and labeled for each mooring.

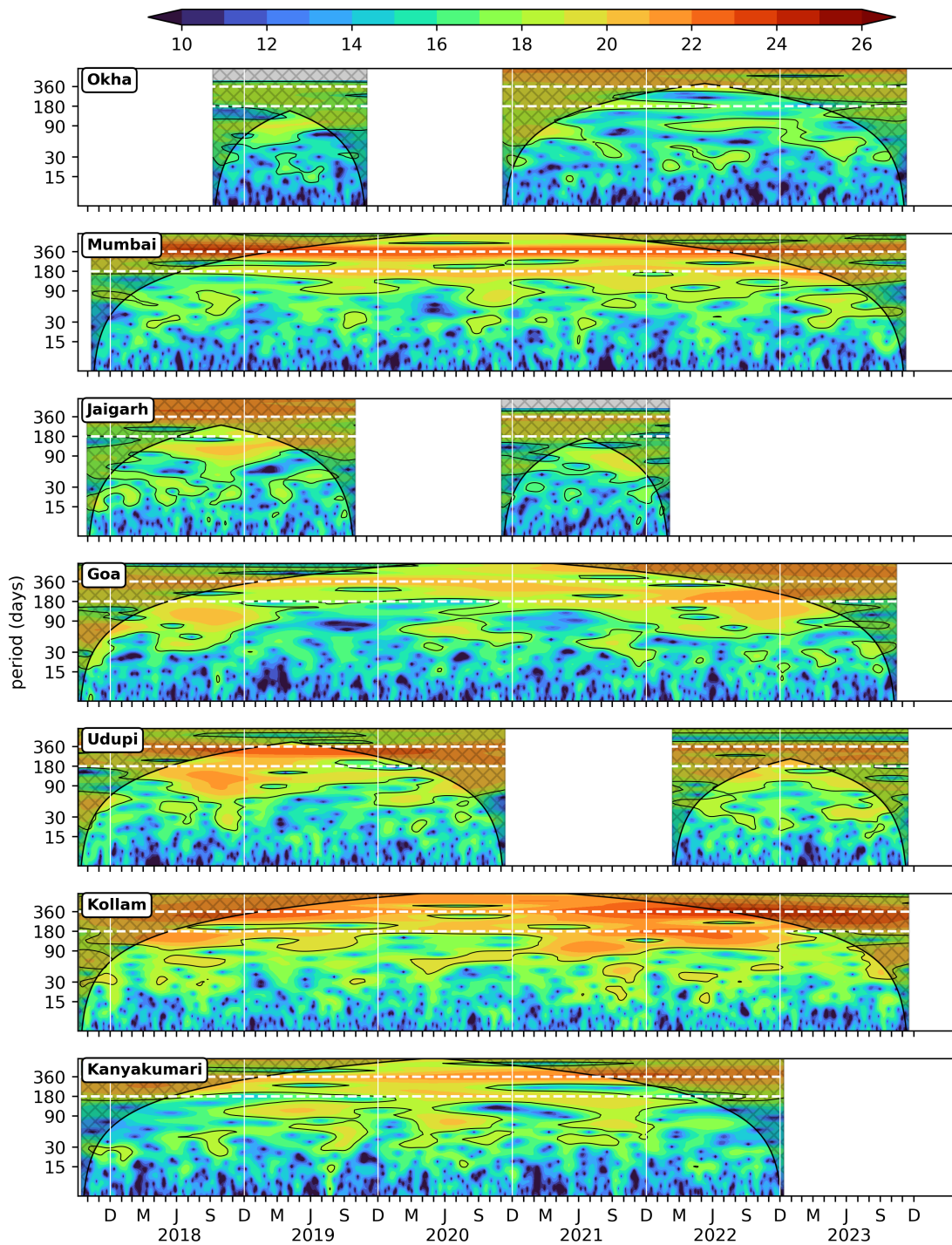


Figure 6: Wavelet power spectra (Morlet) of the 40 m zooplankton biomass plotted against time as abscissa and period in days as ordinate. The wavelet power is in  $\log_2$  scale, the 95 % significance is marked in black contours; the cross-shaded region falls under cone of influence.

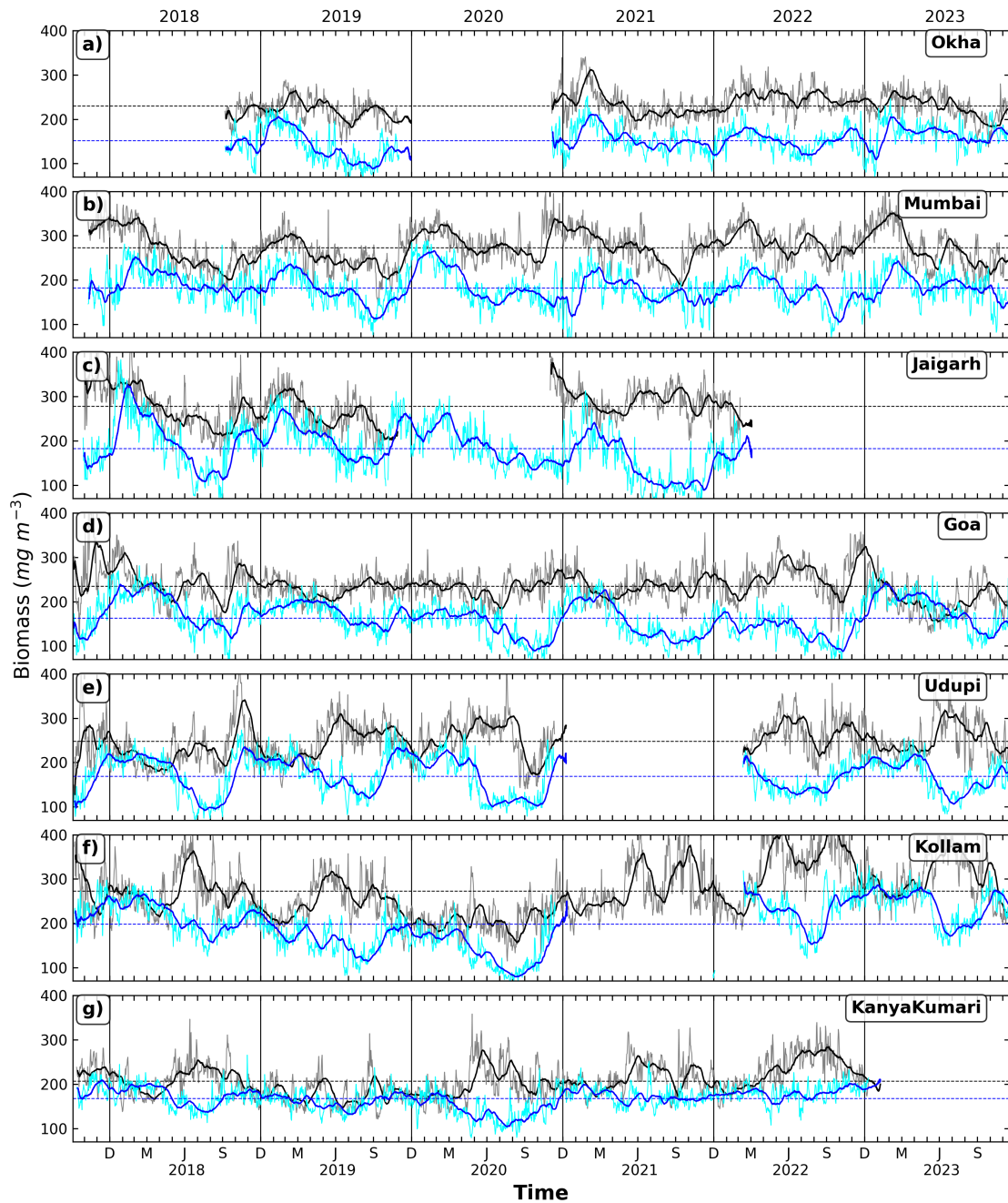


Figure 7: The daily biomass at depth of 40 m and 104 m for all locations shown by grey and cyan curves. The black and blue lines shows the 30 day rolling averaged biomass.